Analysis of EMAA Splats on Glass and Mild Steel Substrates

Wei Xie, James Wang, and Christopher C. Berndt

Thermal spray coatings are composed of millions of heated particles driven at high velocities onto a substrate, thereby building up and forming a consolidated coating. Thus, investigating single solidified droplets contributes to the fundamental understanding of the evolution of a surface coating and its properties. In this study, the single splat morphology and thermal characteristics of flame-sprayed ethylene methacrylic acid (EMAA) splats, deposited at various stand-off distances onto glass and mild steel substrates, are investigated using scanning electron microscopy, differential scanning calorimetry, and thermal gravimetric analysis. This study indicates that the microstructure of EMAA coatings can be controlled by judicially selecting the thermal spray parameters rather than by using the trial and error methods that are often used at present.

Keywords	EMAA, morphology, single splat, stand-off distance, thermal spray

1. Introduction

Surface coatings play a significant role in manufacturing industries due to continuous improvements in their properties that lead to longer service life and reliability. Thermal spray processes, especially of polymeric materials under atmospheric conditions, holds a unique position in the family of available surface engineering technologies since coatings in excess of 20 μm can be deposited over large areas at high deposition rates (Ref 1). The maximum thickness deposited by plasma spray was reported to be 50.8 mm (Ref 2). However, thick coatings have technical concerns since substantial residual stresses may evolve and these need to be controlled by substrate cooling. Such processing needs are critical considerations for the implementation of thermal spray, especially when they exhibit advantages over alternative methods such as electroplating, physical vapor deposition (PVD), and chemical vapor deposition (CVD) (Ref 3).

Polymers can be thermal sprayed by flame spray (FS) (Ref 4-6), plasma spray (Ref 7-9), high velocity oxygen fuel (HVOF) (Ref 10-12), high velocity air fuel (Ref 1), and cold spray (Ref 13) processes; processes which are selected on the basis of the physical properties of the polymer. The FS process exhibits some advantages over plasma spray and HVOF even for high melting polymers, such as polyetheretherketone (PEEK) that melts at 343 °C. Polymer fusion occurs when the preheating temperature and the heat input are appropriately selected due to the lower flame enthalpy and lower stagnation pressure compared to the plasma or HVOF (Ref 14) processes. FS can be used to fabricate denser and smoother PEEK coatings with less porosity and unmelted particles compared with those prepared by plasma and HVOF processes (Ref 1). The ethylene methacrylic acid (EMAA) copolymer containing sodium ions is a common polymer that can be flame sprayed (Ref 15). Such polymers adhere well to steel and aluminium (Ref 16), and withstand high humidity and low temperatures (Ref 17). They are, therefore, widely applied for coating pipes, ladder racking, structural steels, bridges, handrails, screw propellers, wastewater clarifiers, light poles, and many other diverse applications where high chemical resistance and high impact resistance are required (Ref 6, 16, 17).

The coating formation process is generally determined by the prime processing variables, which include substrate roughness, substrate temperature, impact velocity, stand-off distance (SOD), and nature of the local atmospheric environment (Ref 2, 18-20). Many of these factors are inter-related. For example, SOD will influence impact velocity as well as substrate temperature due to heat transfer from the thermal spray torch. The above processing variables influence the physical nature of the intrinsic building blocks of thermal spray coatings; i.e., the splat morphology (Ref 21, 22). Physical behavior, such as thermal conductivity and wetting ability at impact between the thermal-sprayed particle and the substrate, influences the individual splat geometry and coating build-up and, consequently, the coating properties.

The current work seeks to understand the effect of processing parameters on the metrology of splats by focusing on the SOD spray variable. The metrology of

Wei Xie, James Wang, and **Christopher C. Berndt**, IRIS, Faculty of Engineering and Industrial Sciences, Swinburne University of Technology, PO Box 218, Hawthorn, VIC 3122, Australia; and **Christopher C. Berndt**, Department of Materials Science and Engineering, Stony Brook University, Stony Brook, NY 11794. Contact e-mails: xie_samuel@yahoo.com.au, jawang@swin.edu.au, and cberndt@swin.edu.au.

splats, such as the circularity; splat diameter; flattening ratio; degree of splashing; splat and splash size distribution; and the target efficiency are the focus of the current study that aims to derive empirical relationships between SOD and splat morphology. Differential scanning calorimetry (DSC) and thermogravimetric analysis (TGA) of EMAA are carried out to understand the thermal properties.

2. Experimental

The spray process was performed with a Powder Pistol 124 PFS (Thermoplastic Powder Coatings, Big Spring, TX) that is typical of an industrial setting. The combustion gas was a propane/air mixture in the ratio of 1:2 at a flow rate of 40 L/min with the propane adjusted to 0.1 MPa (Ref 23).

A Tecflo 5102 powder feeder was used to spray single splats. The direction of droplet deposition was perpendicular to the substrate surface. A much reduced feedstock delivery rate was necessary; only one traverse with a traverse speed of 25 cm/s across the substrate was performed to achieve single splats that did not overlap. It can be argued that these processing conditions do not accurately represent industrial settings since typical industrial spray parameters would rule out the creation of non-overlapping splats. However, the authors wish to point out that the intent of the present study is to form single, individual splats for scientific observations.

The EMAA, purchased from Innotek Powder Coatings, LLC, exhibited a particle size range from 30 to 400 μm and an angular morphology, as expected from the cryogenic grinding process used to manufacture the powders (Ref 23). The mild steel substrates of 20 × 30 mm area and 2 mm thick were polished using silicon carbide sand paper and diamond compound to achieve a 0.2 μm finish, whereas the glass slides were used in the as-received condition and were of average roughness 0.02 μm.

The size of particles and splats were measured by image analysis software OLYSIA m3 (OLYMPUS®) installed on a Leica MEF4M optical microscope. The deposit morphology was examined through both secondary electron and backscattered electron images using scanning electron microscopy (ZEISS SUPRA 40VP FESEM). The backscattered electron images provided an improved definition between polymer splats and the substrates (Ref 24). The degree of splashing with respect to its circularity was analyzed with image analysis software ImageJ (version 1.43) (Ref 25). The splat area was calculated by summing the pixels, which had been calibrated to an area dimension. Each digital image revealed 70 to 30 splats at 20 and 35 cm SOD, respectively, and at 50× magnifications. In excess of 100 splats were examined for each thermal spray condition. The thermal characteristics were examined using DSC and thermal gravimetric analysis.

Several terms are used throughout this work and they are now formally defined as represented in Table 1.

Table 1 Taxonomy of splats

Taxonomy of splats	Top view	Cross section view
Semi-melted spherical splat		
Resolidified spherical splat		
Disk splat		
Splashed splat		
Splash fragment		

A 'deposit' is a general description for a coating material that is observed on a substrate. A deposit may consist of a 'splat' or a 'splash', or a combination of these features. A splat is described as a deposit that maintains approximately the same volume as the original feedstock powder particle; i.e., it obeys conservation of volume principles. A splash does not obey such physical principles and appears fragmented in appearance. Within this taxometric definition, 'flower petal' structures might be classified as splats, however, they are better described as exhibiting a splash morphology due to the highly fragmented nature. Thus, the transformation of a splat to a splash morphology is correlated to the ratio of the perimeter to the surface area of the microstructural artifact.

There are additional terms of 'unmelted splat' and 're-solidified splat' used within the present contribution. An unmelted splat refers to particles that are partially melted and retain the near-spherical morphology of the feedstock material, whereas a 're-solidified splat' represents melted particles that have re-solidified and also maintain the near-spherical morphology of the feedstock material. Unmelted splats and re-solidified splats are reflective of a low processing temperature brought about by either small or large SODs, respectively.

3. Results and Discussion

3.1 Differential Scanning Calorimetric and Thermogravimetric Analysis of EMAA

Figure 1 shows the thermal characteristics obtained by conducting differential thermal analysis and TGA under air and nitrogen atmospheres. The melting temperature and vaporization temperature of EMAA were 100 and 410 °C, respectively, under either air or nitrogen atmospheres. The EMAA decomposition temperature of 330 °C in air may be associated with oxidation, however, there was no decomposition or oxidation of EMAA under a nitrogen atmosphere. Thus, the process temperature of EMAA in air was chosen from 100 to 330 °C and it is reasonable to expect that EMAA can be flame sprayed at 410 °C in nitrogen environments at atmospheric pressures. The particle temperature at impact varies from 100 to 330 °C according to the four different SOD.

3.2 Influence of Spray Distance on Splat Circularity

Figure 2 depicts the percentage of splats and splashes of EMAA deposited onto the glass and the mild steel substrates. The assumption of a deposition efficiency of 100% should be challenged. Recall that a splat refers to a pan cake-shaped deposit, while a splash exhibits an irregular and non-circular geometry with fingers and other protuberances that may be connected or within the vicinity of a central mass of the coating material (Ref 26). Thus, a typical spray attribute for polymers sprayed under a broad range of conditions is 100%. However, within the context of this current work where atypical conditions are
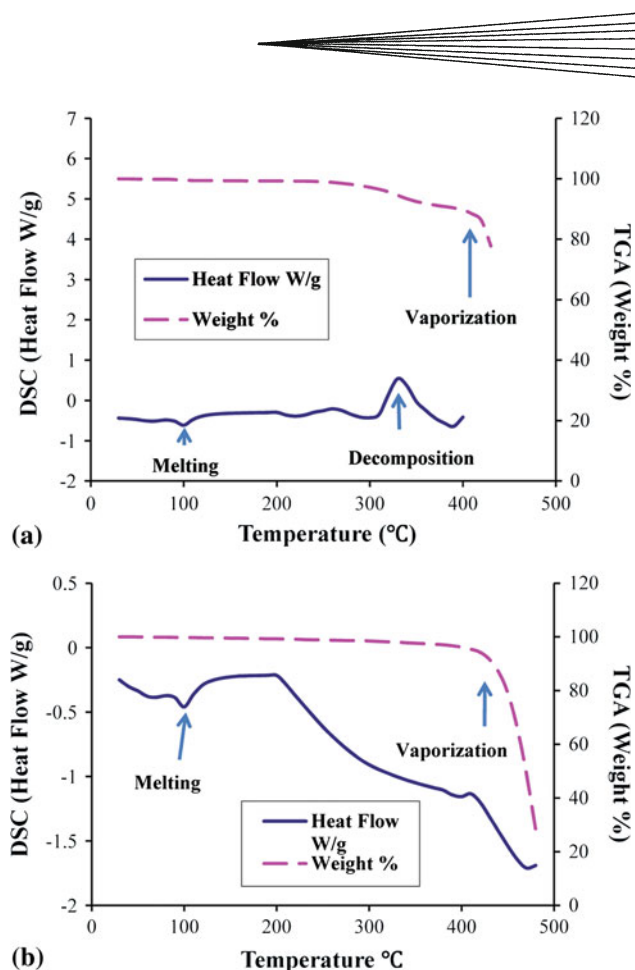

Fig. 1 Differential scanning calorimetric and thermogravimetric analysis of EMAA in air (a) and in nitrogen (b)

being explored so that different deposit morphologies can be created, the deposition efficiency is likely to be less than 100%. Therefore, care needs to be exercised when interpreting Fig. 2 since the splat and splash morphologies may have different feedstock pedigrees.

Figure 2(a) indicates that splash behavior can be minimized at a SOD of 35 cm for the glass substrates. However, at the same SOD, 7% of the deposits sprayed onto steel substrates demonstrate a splash morphology, as shown in Fig. 2(b). In general, increasing SOD to 35 cm results in the formation of disk-shaped splats. A higher percentage of the splash morphology was observed on mild steel substrates than glass substrates (Ref 23, 26, 27). It is suggested that more rapid freezing occurs on mild steel than on glass substrates due to the higher thermal conductivity of the steel (Ref 28). The thermal conductivity of the mild steel and glass substrates are 36-54 and 1.09-1.2 W/m/K (Ref 29, 30), respectively, thus the thermal diffusivity of the mild steel is higher than that of the glass substrates. The solidification of the splat bottom impedes the liquid flow and results in splashing. Therefore, in instances where splats are the preferred morphology then the mild steel substrate should be preheated (Ref 21, 22, 31).

Large area SEM images of the deposits under low magnification verified that the deposition efficiency was
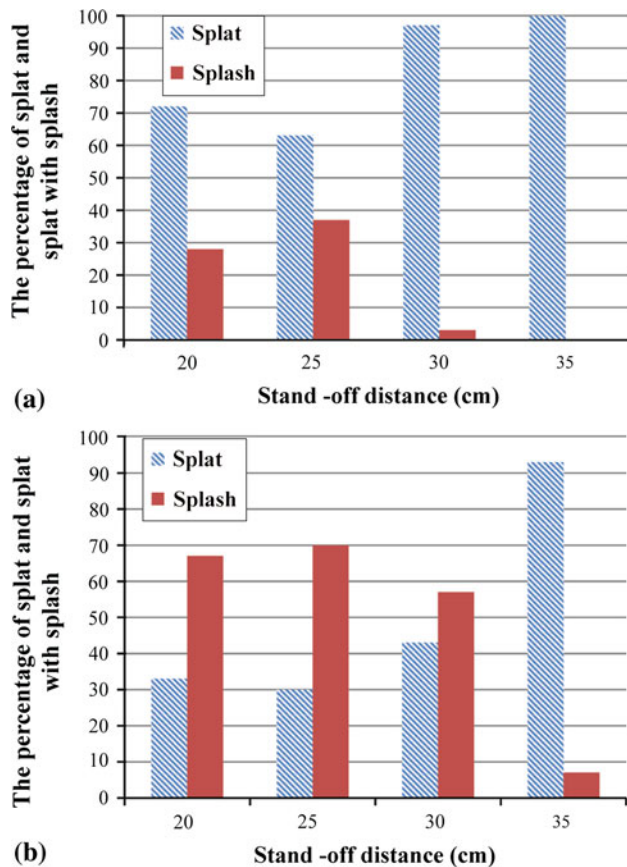
Fig. 2 The effect of stand-off distance on the morphology of EMAA on glass (a) and mild steel substrates (b)

Fig. 3 The effect of stand-off distance on the diameter of EMAA single splats on glass (a) and mild steel substrates (b)

reduced and more resolidified splats were observed at SOD greater than 30 and 35 cm for glass and mild steel substrates, respectively (Ref 23). The particle temperature would be reduced after traversing 30 cm SOD; thus some of those particles may be resolidified. As well, some particles may not deposit on the target due to non-optimal trajectories; thus causing the DE to be reduced. The result that a SOD difference of 5 cm can influence the quality of a coating (or splat, in the case of the present work) has important implications. Therefore, an application that requires coverage over two abutting materials of dissimilar characteristics, such as thermal conductivity, will require special spray protocols that account for these conflicting spray parameters.

3.3 Spray Distance Effect on Splat Diameter and the Flattening Ratio

Splat diameter versus SOD is depicted in Fig. 3. Splat diameter is the diameter of a disk splat. The maximum flattening ratio can be achieved at SOD of 30 and 25 cm, respectively, by depositing EMAA onto the glass and the mild steel substrates. It should be recalled that in excess of 100 splats were measured for these data points. Figure 3(a) demonstrates that the diameter of splats deposited onto the glass substrate increased from 180 to
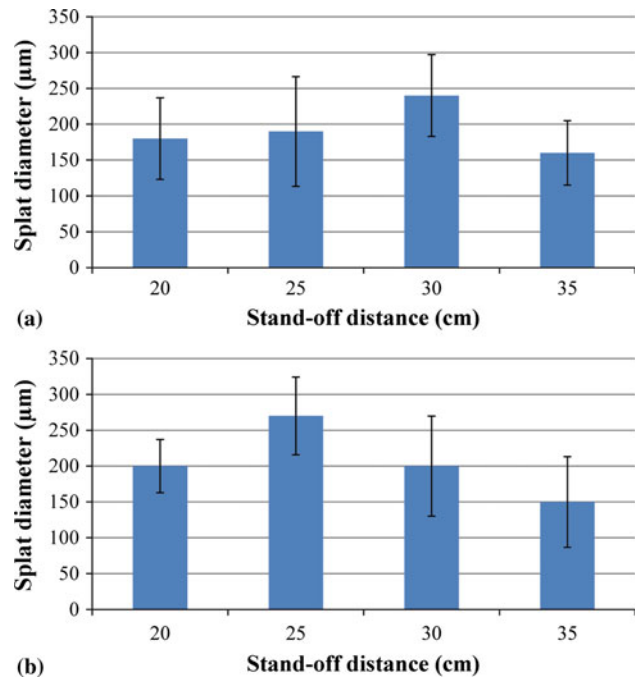
240 μm when the SOD increased from 20 to 30 cm and reduced to 160 μm when SOD increased by a further 5 to 35 cm. To state this result in another way: 'A 17% increase in the SOD reduced the splat diameter by 50%'.

A similar effect was also observed for the mild steel substrate, Fig. 3(b), yet in this instance the splat diameter was much less sensitive to SOD. The splat diameters on the mild steel substrate increased from 200 to 270 μm when the SOD increased from 20 to 25 cm and reduced to 150 μm with a further SOD increase to 35 cm.

The flattening ratio is defined as the splat diameter to the original molten droplet diameter (Ref 28, 32, 33). The flattening ratio is a measure for the degree of particle deformation. The EMAA particle size is considered as the original molten droplet diameter. Figure 4(a) indicates that the flattening ratio, ξ, of splats on glass increased from 1.29 to 1.71 at SOD of 20 to 30 cm and decreased to 1.14 at 35 cm SOD. Figure 4(b) shows that ξ of splats on mild steel substrates increased from 1.43 to 1.93 at 20 to 25 cm SOD and decreased to 1.07 at 35 cm SOD.

The results demonstrate that the maximum flattening ratio was achieved at SOD of 30 and 25 cm, respectively, by depositing EMAA onto the glass and the mild steel substrates, as shown in Fig. 4. The results indicate that the highest splat temperatures arise at SODs of 30 cm on the glass and 25 cm on the mild steel substrates due to the higher thermal conductivity of mild steel substrates than that of the glass substrates. The SOD influences the splat temperatures independent of substrate. The splat temperatures affect the flattening ratio; i.e., the higher the temperature of splats on the substrates, the higher the flattening ratio. The data also demonstrate that spraying

onto a glass substrate is a more sensitive process that would require careful control of the SOD to achieve the optimum splat morphology.

3.4 Spray Distance Effect on Target Efficiency

Deposition efficiency (DE), expressed as a percentage, is defined as the weight of spray deposit to the weight of the material sprayed (Ref 34). DE provides a measure for optimizing the process parameters. High DE is desirable and critical. Low DE suggests that some coarse or fine powders are not being deposited. When substrate geometry, size, and over spray are taken into consideration, the DE may be reduced significantly and cause a low yield on the component. The relative amount of material that eventually deposits onto a practical substrate is termed as the 'target efficiency' (TE).

The DE here should be termed as the target efficiency (Ref 35) since the mild steel substrate dimensions are 20×30 mm instead of 300×300 mm according to the DE determination standard (Ref 36). Figure 5 shows the SOD effect on the TE of mild steel substrates. The TE is 5, 3, 2.2, and 1.7% at 20, 25, 30, and 35 cm SOD, respectively, and indicates a decline with increasing SOD. It is cautioned that the target efficiencies reported in this work are abnormally and artificially lower than those experienced within industry since the powder feed rate has been lowered by a factor of 10 to form deposits that permitted scientific analysis.

Within the context of the present study the target efficiency analysis implies that optimum deposit morphology appears as a splat rather than a splash. Such an analysis is of benefit in estimating cost and powder consumption for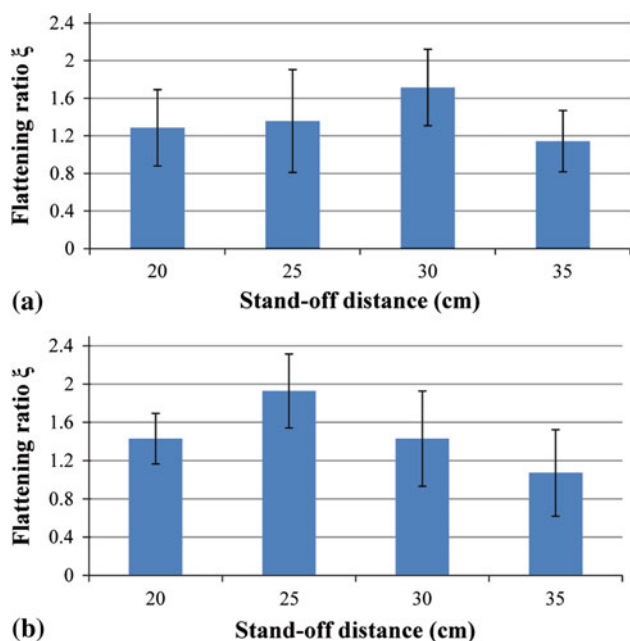 manufacturing applications. An important caution concerns the assumption that the greatest TE or DE also supports the optimum extrinsic material properties of the coating. This conjecture has not been validated for thermal spray deposits.

3.5 Particle, Splat, and Splash Size Distribution on Mild Steel at 25 cm Spray Distance

Figure 6 shows the particle, splat, and splash deposit size frequency distributions on mild steel substrates at 25 cm SOD. These distributions have been normalized and appropriate class intervals selected so that data comparisons can be performed. The mono-modal distributions indicated in Fig. 6 can be used to carry out simple calculations concerning the transformation of spherical feedstock particles to splats or splashes represented as squat column structures; i.e., assuming a circular footprint and regular height in the disk shape. The particle mode at 100 μm can transform either to (i) a spat that is of 16.7 μm height (200 μm diameter) and a flattening ratio of 2, or (ii) a splash of 13.2 μm height (225 μm diameter) and a flattening ratio of 2.25.

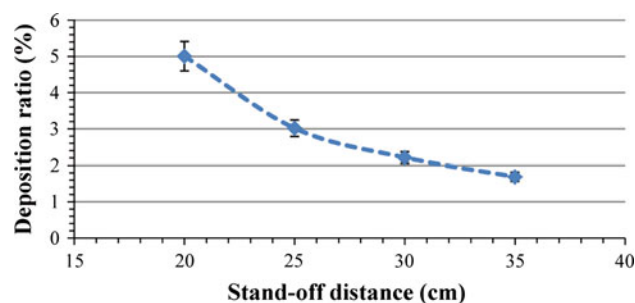**Fig. 5** SOD effect on target efficiency of mild steel substrates

Fig. 4 The effect of stand-off distance on the flattening ratio ξ of EMAA single splats on glass (a) and mild steel substrates (b)
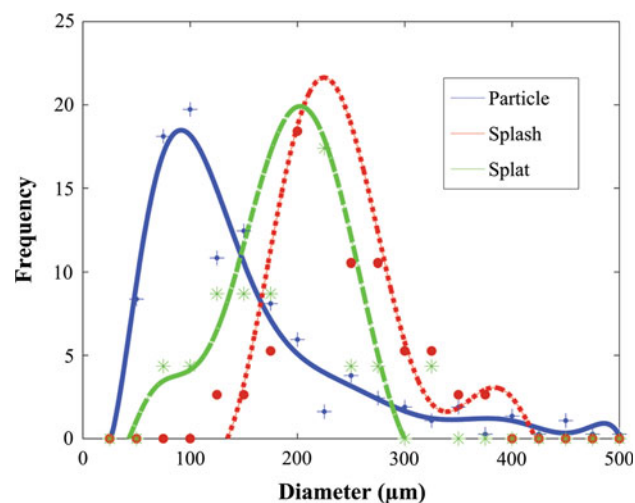
Fig. 6 Particle, splat, and splash size distribution on mild steel at 25 cm SOD

In general terms, the mode value of splat and splash deposits were shifted to greater sizes of 200 and 225 μm with respect to the 100 μm diameter of the feedstock.

3.6 Spray Distance Effect on the Size Distribution of Splat and Splashed Splat on Mild Steel

Figure 7 shows the SOD effect on the size distribution of splats (Fig. 7a) and splashes (Fig. 7b) deposited onto mild steel substrates. The distributions reveal primarily mono-modal distributions (Fig. 7a). The mode values of the splat diameters are 200, 250, 200, and 150 μm at SODs of 20, 25, 30 and 35 cm, respectively. Figure 7(b) shows that the mode of splash diameter is 200, 250, and 350 μm at corresponding SODs of 20, 25, and 30 cm.

Degree of splashing (DS) is the ratio of the area of a splashed splat to that of the disk splat, where P is the splash perimeter and A is the area of the disk-like splat. When DS = 1, (Ref 37)

$$DS = \frac{1}{4\pi} \cdot \frac{P^2}{A} \qquad (Eq\ 1)$$

then the splat morphology is a perfect disk. The higher the DS, the more fingered or fragmented the splats. The DS in this paper is calculated from the circularity metric. Circularity is the ratio of the area of a splat to that of the splash. Thus DS = 1/circularity. The (Ref 24) circularity data,

$$Circularity = \frac{4\pi A}{P^2}, \qquad (Eq\ 2)$$

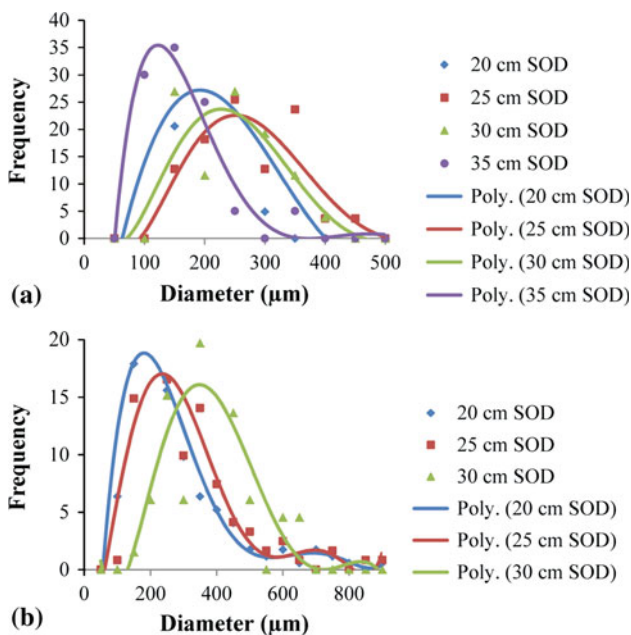from this research are acquired from Imagej software. The splats counted here are splashed splats. The DS of all splat morphologies at 35 cm SOD could not be resolved sufficiently by using optical microscopy techniques. The low flame temperature at a long SOD resulted in the re-solidification of melted particles.

Figure 8 shows the variation of DS on glass and mild steel substrates, respectively. Generally the DS on glass substrates is smaller than that on mild steel substrates due to the lower thermal conductivity of glass in comparison to that of mild steel. The degree of splashing on glass substrates decreases from 3.61 (at 20 cm SOD) to 3.12 (at 25 cm SOD), and from 3.23 (at 30 cm SOD) to 1.70 (at 35 cm SOD). The lowest DS is found at 25 cm SOD. The DS on mild steel substrates increases from 4.50 to 5.40, and then decreases from 3.76 to 3.49 at SOD from 20 to 35 cm. The minimum DS occurs at 30 cm SOD. The highest DS is at 25 cm SOD, as the EMAA particles at 25 cm SOD have higher temperature and velocity. The observed results are in good agreement with the analysis on splat circularity discussed previously.

3.7 FTIR Spectra Analysis of EMAA Coatings

Figure 9 shows FTIR spectra of EMAA coatings sprayed with a Powder Pistol 124 PFS (Thermoplastic Powder Coatings, Big Spring, TX, USA) and Tecflo 5102 fluidized bed powder feeder at 20, 25, 30, and 35 cm SODs with liquid propane gas (LPG) as a fuel. There was no marked change in the intensity of the peaks between powders and coatings, indicating that there was no deterioration of EMAA during the FS process.
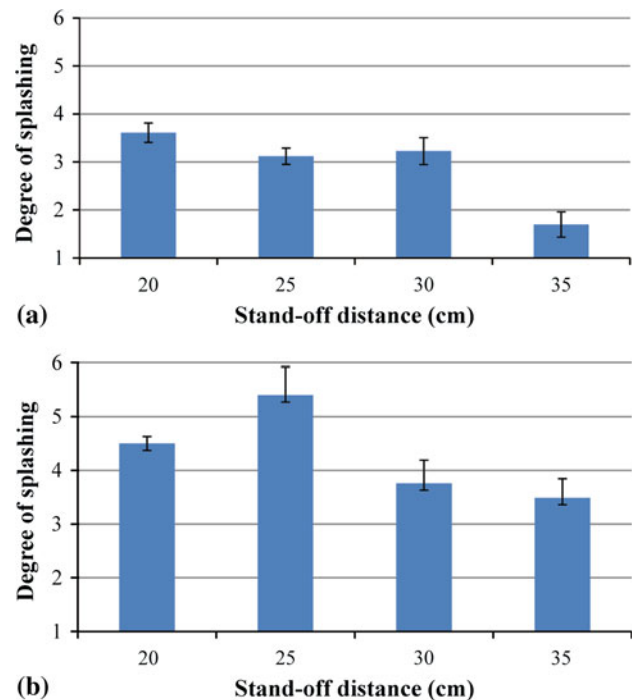

Fig. 7 SOD effect on the size distribution of disk splat (a) and splash splat (b) on mild steel substrates

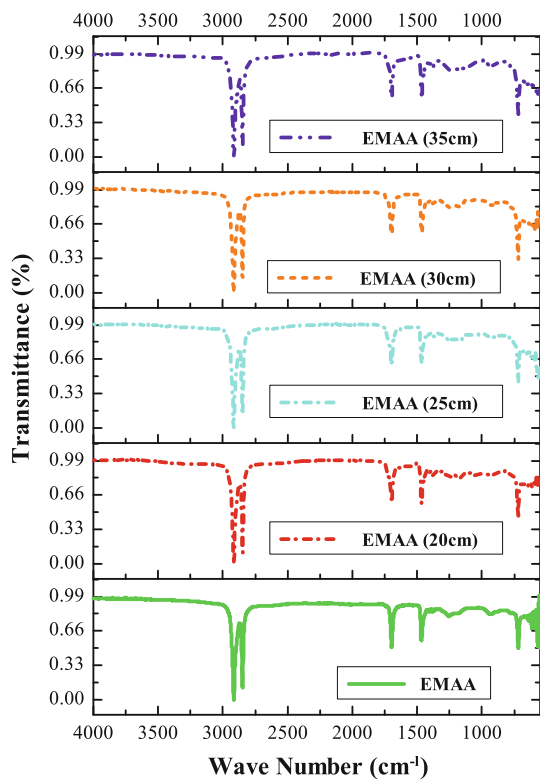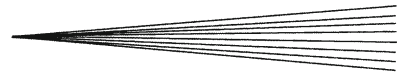**Fig. 8** SOD effect on degree of splashing on glass (a) and mild steel substrates (b)

Fig. 9 FTIR spectra of EMAA coatings at different stand-off distances (LPG)

4. Conclusions

Single splats were examined since these are the basic building blocks of any thermal spray coating. Therefore, it is important to point out that the thermal spray process was not optimized since the primary aim focused on understanding the whole processing envelope.

The flattening ratio of single splats increases with the SOD up to 30 cm on glass substrates and 25 cm on steel substrates, at greater SODs the flattening ratio decreases. The mode value of the diameter of splat and splash shifts to greater sizes than the sizes of feedstock particles. The target efficiency of EMAA decreases dramatically with an increase of SOD. Increasing SOD results in more spherical splats. This study provides practical guidance concerning the nature of how prime spray variables influence processing/morphology relationships.

The FTIR of EMAA coatings indicated that there was no detectable deterioration of the EMAA feedstock during the FS process.

References

1. E. Petrovicova and L.S. Schadler, Thermal Spraying of Polymers, *Int. Mater. Rev.*, 2002, **47**(4), p 169-190
2. G.K. Sweet, Applying thermoplastic/thermoset powder with a modified plasma system, *Thermal Spray Coatings: Research, Design and Applications*, C.C. Berndt and T.F. Bernecki Eds., June 7-11, 1993, ASM International, Anaheim, CA, 1993, p 381-384
3. S. Kuroda, J. Kawakita, M. Watanabe, and H. Katanoda, Warm Spraying-A Novel Coating Process Based on High-Velocity Impact of Solid Particles, *Sci. Technol. Adv. Mater.*, 2008, **9**(3), p 1-17
4. J.A. Brogan, "Processing and Property Relationships of Thermally Sprayed Polymer Systems," Ph.D. Thesis, State University of New York, 1996
5. J.A. Brogan, and C.C. Berndt, The mechanical properties of combustion-sprayed polymers and blends, *Thermal Spray: Practical Solutions for Engineering Problems*, C.C. Berndt Ed., ASM International, Cincinnati, Ohio, 1996, p 221-226
6. J.A. Brogan and C.C. Berndt, The Coalescence of Combustion-Sprayed Ethylene-Methacrylic Acid Copolymer, *J. Mater. Sci.*, 1997, **32**(8), p 2099-2106
7. Y. Bao, D.T. Gawne, D. Vesely, and M.J. Bevis, Production of Polymer Matrix Composite Coatings by Thermal Spraying, *Trans. Inst. Metal Finish.*, 1994, **72**(pt 3), p 110-113
8. Y. Bao, D.T. Gawne, and T. Zhang, Effect of Feedstock Particle Size on the Heat Transfer Rates and Properties of Thermally Sprayed Polymer Coatings, *Trans. Inst. Metal Finish.*, 1995, **73**(pt 4), p 119-124
9. Y. Bao, D.T. Gawne, D. Vesely, and M.J. Bevis, Formation and Microstructure of Plasma Sprayed Polyamide Coatings, *Surf. Eng.*, 1994, **10**(4), p 307-313
10. T. Twardowski, M. Reilly, and R. Knight, Properties of HVOF sprayed multi-scale polymer/silica nanocomposite coatings, *Thermal Spray 2001: New Surfaces for a New Millenium*, C.C. Berndt, K.A. Khor and E.F. Lugscheider Eds., ASM International, Singapore, 2001, p 369-373
11. E. Petrovicova, R. Knight, R.W. Smith, and L.S. Schadler, Structure and properties of HVOF sprayed ceramic/polymer nano-composite coatings, *Thermal Spray: A United Forum for Scientific and Technological Advances*, C.C. Berndt Ed., ASM International, Indiannapolis, Indiana, 1997, p 877-883
12. E. Petrovicova, R.W. Smith, R. Knight, and L.S. Schadler, Particulate Nanoreinforced Polymer Composites Processing and Properties, *J. Therm. Spray Technol.*, 1998, **7**(3), p 426-427
13. Y. Xu and I.M. Hutchings, Cold Spray Deposition of Thermoplastic Powder, *Surf. Coat. Technol.*, 2006, **201**(6), p 3044-3050
14. H. Liao, E. Beche, F. Berger, and C. Coddet, On the microstructures of thermally sprayed "PEEK" polymer, *Thermal Spray: Meeting the Challenges of the 21st Century*, C. Coddet Ed., May 25-29, ASM International, Nice, France, 1998, p 25-30
15. J.A. Brogan, R. Lampo, and C.C. Berndt, Thermal Spraying of polymers, *Fourth World Congress on Coating Systems for Bridges and Steel Structures*, 1995, p 200
16. P.J. Loustaunau and D. Horton, EMAA Thermoplastic Powder Coatings in Shop and Field Applications, *Mater. Perform.*, 1994, **33**(7), p 32-36
17. T.W. Glass, and J.A. Depay, Thermal spray coatings: properties, processes and applications, *The Fourth National Thermal Spray Conference*, T.F. Bernecki Ed., May 4-10, ASM International, Pittsburgh, Pennsylvania, 1991, p 345-351
18. A. Vardelle, C. Moreau, and P. Fauchais, The Dynamics of Deposit Formation in Thermal-Spray Processes, *MRS Bull.*, 2000, **25**(7), p 32-37
19. M. Bussmann, S. Chandra, and J. Mostaghimi, Modeling the Splash of a Droplet Impacting a Solid Surface, *Phys. Fluids*, 2000, **12**(12), p 3121-3132
20. H. Herman, S. Sampath, and R. McCune, Thermal Spray: Current Status and Future Trends, *MRS Bull.*, 2000, **25**(7), p 17-25
21. P. Fauchais, M. Fukumoto, A. Vardelle, and M. Vardelle, Knowledge Concerning Splat Formation: An Invited Review, *J. Therm. Spray Technol.*, 2004, **13**(3), p 337-360

22. S. Sampath, X.Y. Jiang, J. Matejicek, A.C. Leger, and A. Vardelle, Substrate Temperature Effects on Splat Formation, Microstructure Development and Properties Of Plasma Sprayed Coatings Part I: Case Study for Partially Stabilized Zirconia, *Mater. Sci. Eng. A*, 1999, **272**(1), p 181-188

23. W. Xie, J. Wang, and C.C. Berndt, Spreading Behavior and Morphology of Ethylene Methacrylic Acid (EMAA) Deposits via the Flame Spray Process, *Coatings*, 2012, **2**(2), p 76-93

24. B.P. Withy, M.M. Hyland, and B.J. James, *The Effect of Surface Chemistry and Morphology on the Properties of HVAF PEEK Single Splats*, Springer, 2008, p 631-636

25. W.S. Rasband, ImageJ, U.S. National Institutes of Health, 1997-2010

26. W. Xie, S. Saber-Samandari, J. Wang, and C.C. Berndt, Effect of stand-off distance on EMAA splats deposited onto glass and mild steel substrates, *ITSC2010*, 2010 (Singapore), DVS-German Welding Society, ASM International-Thermal Spray Society (TSS), IIW-International Institute of Welding, 2010, p 559

27. W. Xie, J. Wang, and C.C. Berndt, Ethylene Methacrylic Acid (EMAA) Single Splat Morphology, *Coatings*, 2013, **3**(2), p 82-97

28. X. Jiang, J. Matejicek, and S. Sampath, Substrate Temperature Effects on the Splat Formation, Microstructure Development and Properties of Plasma Sprayed Coatings Part II: Case Study for Molybdenum, *Mater. Sci. Eng. Struct. Mater. Prop. Microstruct. Process.*, 1999, **272**(1), p 189-198

29. D.R. Lide, CRC *Handbook of Chemistry and Physics*, CRC Press, Boca Raton, 1995

30. A. Bejan, and A.D. Kraus, *Heat Transfer Handbook*, Wiley Inc., Hoboken, 2003

31. L. Bianchi, A. Grimaud, F. Blein, P. Lucchese, and P. Fauchais, Comparison of Plasma-Sprayed Alumina Coatings by RF and DC Plasma Spraying, *J. Therm. Spray Technol.*, 1995, **4**(1), p 59-66

32. S. Amada, K. Tomoyasu, and M. Haruyama, Splat formation of molten Sn, Cu and Ni droplets, *Surf. Coat. Technol.*, 1997, **96**(2-3), p 176-183

33. A. Kucuk, C.C. Berndt, U. Senturk, and R.S. Lima, Influence of Plasma Spray Parameters on Mechanical Properties of Yttria Stabilized Zirconia Coatings. II: Acoustic Emission Response, *Mater. Sci. Eng. A*, 2000, **284**(1-2), p 41-50

34. F.J. Hermanek, *Thermal spray technology and company origins,* ASM International, Materials Park, 2001

35. J.R. Davis, *Handbook of Thermal Spray Technology*, ASM International, Materials Park, 2004, p 338

36. BSI, *Thermal Spraying-Determination of the Deposition Efficiency for Thermal Spraying*, European Committee for Standardization, 2004, p 1-10

37. G. Montavon, S. Sampath, C.C. Berndt, H. Herman, and C. Coddet, Effects of the Spray Angle on Splat Morphology During Thermal Spraying, *Surf. Coat. Technol.*, 1997, **91**(1-2), p 107-115